Rapid scanning of spin noise with two free running ultrafast oscillators

Jens Hübner,[*] Jan Gerrit Lonnemann, Petrissa Zell, Hendrik Kuhn, Fabian Berski, and Michael Oestreich

Institute for Solid State Physics, Leibniz University Hannover, Appelstr. 2, 30167 Hannover, Germany
[*]*jhuebner@nano.uni-hannover.de*

Abstract: We combine the scanning temporal ultrafast delay (STUD) technique with spin noise spectroscopy (SNS), which is based upon below band gap Faraday rotation to investigate the full temporal dynamics of stochastically orientated electron spins in slightly n-doped bulk GaAs. The application of STUD-SNS boosts the common technical bandwidth limitation of the electro-optic conversion in cw-SNS into the several hundred GHz regime. Numerical simulations highlight the strengths and examine the limitations of STUD-SNS.

References and links

1. G. M. Müller, M. Oestreich, M. Römer, and J. Hübner, "Semiconductor spin noise spectroscopy: Fundamentals, accomplishments, and challenges," Physica E **43**(2), 569–587 (2010).
2. R. Kubo, "The fluctuation-dissipation theorem," Rep. Prog. Phys. **29**(1), 255–284 (1966).
3. M. Römer, H. Bernien, G. Müller, D. Schuh, J. Hübner, and M. Oestreich, "Electron-spin relaxation in bulk GaAs for doping densities close to the metal-to-insulator transition," Phys. Rev. B **81**(7), 075216 (2010).
4. G. M. Müller, M. Römer, J. Hübner, and M. Oestreich, "Gigahertz spin noise spectroscopy in n-doped bulk GaAs," Phys. Rev. B **81**(12), 121202 (2010).
5. G. M. Müller, M. Römer, D. Schuh, W. Wegscheider, J. Hübner, and M. Oestreich, "Spin noise spectroscopy in GaAs (110) quantum wells: Access to intrinsic spin lifetimes and equilibrium electron dynamics," Phys. Rev. Lett. **101**(20), 206601 (2008).
6. S. A. Crooker, J. Brandt, C. Sandfort, A. Greilich, D. R. Yakovlev, D. Reuter, A. D. Wieck, and M. Bayer, "Spin noise of electrons and holes in self-assembled quantum dots," Phys. Rev. Lett. **104**(3), 036601 (2010).
7. R. Dahbashi, J. Hübner, F. Berski, J. Wiegand, X. Marie, K. Pierz, H. W. Schumacher, and M. Oestreich, "Heavy-hole spin dephasing in (InGa)As quantum dots," Appl. Phys. Lett. **100**(3), 031906 (2012).
8. M. Wu, J. Jiang, and M. Weng, "Spin dynamics in semiconductors," Phys. Rep. **493**(2-4), 61–236 (2010).
9. I. A. Merkulov, A. L. Efros, and M. Rosen, "Electron spin relaxation by nuclei in semiconductor quantum dots," Phys. Rev. B **65**(20), 205309 (2002).
10. R. I. Dzhioev, K. V. Kavokin, V. L. Korenev, M. V. Lazarev, B. Ya. Meltser, M. N. Stepanova, B. P. Zakharchenya, D. Gammon, and D. S. Katzer, "Low-temperature spin relaxation in n-type GaAs," Phys. Rev. B **66**(24), 245204 (2002).
11. F. Meier and B. P. Zakharchenya, eds., *Optical Orientation* (North-Holland, 1984).
12. F. Bloch, "Nuclear Induction," Phys. Rev. **70**(7-8), 460–474 (1946).
13. I. Žutić, J. Fabian, and S. Das Sarma, "Spintronics: Fundamentals and applications," Rev. Mod. Phys. **76**(2), 323–410 (2004).
14. S. Starosielec and D. Hägele, "Ultrafast spin noise spectroscopy," Appl. Phys. Lett. **93**(5), 051116 (2008).
15. M. Römer, J. Hübner, and M. Oestreich, "Spatially resolved doping concentration measurement in semiconductors via spin noise spectroscopy," Appl. Phys. Lett. **94**(11), 112105 (2009).
16. M. Römer, J. Hübner, and M. Oestreich, "Spin noise spectroscopy in semiconductors," Rev. Sci. Instrum. **78**(10), 103903 (2007).
17. F. Berski, H. Kuhn, J. G. Lonnemann, J. Hübner, and M. Oestreich, "Ultrahigh Bandwidth Spin Noise Spectroscopy: Detection of large g-factor fluctuations in highly n-doped GaAs," arXiv:1207.0081v1.

1. Introduction

Spin noise spectroscopy (SNS) in semiconductors has attracted steadily increasing attention in recent years due to its versatile and yet powerful capabilities for the investigation of the undisturbed spin dynamics in semiconductor nanostructures [1]. The technique relies on the fact that the complete temporal dynamics of a system at thermal equilibrium can be extracted from the noise spectrum of the investigated entity *without* driving the system out of

equilibrium [2]. The excitation pump in traditional optical pump-probe experiments induces spin dephasing mechanism which can overshadow the inherent spin dynamics. However, SNS is an excitation free technique and hence allows the detection of the underlying inherent spin dynamics. Continuous-wave all optical SNS is thus the perfect tool to study undisturbed and therefore long-living spin decoherence processes and has already unveiled a wide range of complex spin interactions in semiconductors and semiconductor nanostructures [3–7]. However, fast decoherence processes correspond to high detection bandwidths and thus the electro-optical conversion dictates the technical limit of the maximum achievable time resolution. An obvious way to avoid this bottleneck is to merge the advantages of ultrafast laser spectroscopy with SNS. The usage of a single pulsed 80 MHz picosecond-laser oscillator has already enabled the extension of the detectable frequencies into the multi GHz regime by stroboscopic probing, i.e., undersampling of the spin dynamics [4]. However, the complete full bandwidth of the electro-optical receivers still puts an upper limit on the detectable spin dephasing rates. In this paper we put forward the connection of spin noise spectroscopy with scanning temporal ultrafast delay (STUD) techniques to completely overcome this limitation. The resulting STUD-SNS method is perfectly tailored to capture the fast spin dynamic of systems which are susceptible to direct optical excitation and the accompanied heating of the carrier systems like, for instance, hole-spin systems [8]. For a general demonstration of the powerful capabilities of STUD-SNS, we have chosen in this publication moderately low n-doped bulk GaAs as a well characterized model system with a sufficiently short spin lifetime.

Spin noise in semiconductors

Spin noise in systems with a finite number of spins [12] – like for instance weakly n-doped GaAs where each localized donor electron represents a quasi independent spin – arises from the statistically incomplete cancellation of up and down spins for any given projection axis. This effective spin polarization at thermal equilibrium gives rise to a Faraday rotation of a transmitted linear light polarization since the two circular light components representing the linear light polarization experience different dispersions due to the optical spin selection rules [11]. The GaAs sample system does not bear a permanent magnetization, i.e., a polarization of the spins, and the stochastic spin polarization decays and builds up on the characteristic timescale given by the specific spin coherence time τ_s. The sample used in this work is Chzochralski grown, bulk GaAs with a nominal n-type Si-doping concentration of $2.7 \cdot 10^{15} \text{cm}^{-3}$ and is about $300\,\mu\text{m}$ thick with both front and back surfaces anti-reflection coated for optimized transmission. The doping concentration is roughly a factor of ten below the metal-to-insulator transition and thus the electrons are partly localized at low temperatures. Localization invokes a pronounced hyperfine interaction with the random local nuclear magnetic field inducing very short spin dephasing times on the order of a few nanoseconds [3,9,10]. Short spin coherence times are expected as well for degenerate binary semiconductors where the doping concentration lies well above the metal-to-insulator transition. In that case, a spin noise signal occurs at finite temperatures due to the fermionic nature of the electronic phase space filling and spin decoherence occurs due to Dyakonov-Perel (DP) spin dephasing [11,13].

2. Technique

The probe light source for the STUD-SNS measurements are two free running picosecond Ti:Sapphire laser oscillators which are slightly detuned in their repetition frequencies $f_r \cong 80$ MHz by $\Delta f \ll f_r$ with all other parameters kept identical. The usage of two free running lasers is an extension to the approach proposed in [14]. with the advantage that the full time dynamic of the investigated system is recorded on a very short timescale ($\sim 1/\Delta f$) and is thus less susceptible to instabilities within the measurement setup.

The experimental setup is depicted in Fig. 1. The optical output of both laser oscillators is coupled into a single mode fiber and joined via a 50:50 fiber splitter to ensure an identical beam profile at the fiber output. The optical fiber is polarization maintaining in order to minimize polarization noise due to thermal stress within the fiber which would translate into excess intensity noise after the linear polarizer at the fiber output. The probe light is focused onto the sample which is mounted in a helium flow cryostat with direct optical access inside the bore of a superconducting magnet. A transverse magnetic field B is used to modulate the stochastic spin polarization with a Larmor frequency $v_L = h^{-1}g*\mu_B B$. Here, h is Planck's constant, μ_B Bohr's magneton, and g^* is the effective Landé g-factor. The polarization rotation of the re-collimated light collected behind the sample is analyzed by a polarization bridge consisting of a linear polarizing Wollaston prism and an 80 MHz balanced photodiode receiver. A λ/2 waveplate in front of the Wollaston prism is used to balance the average light intensity on the two photodiodes.
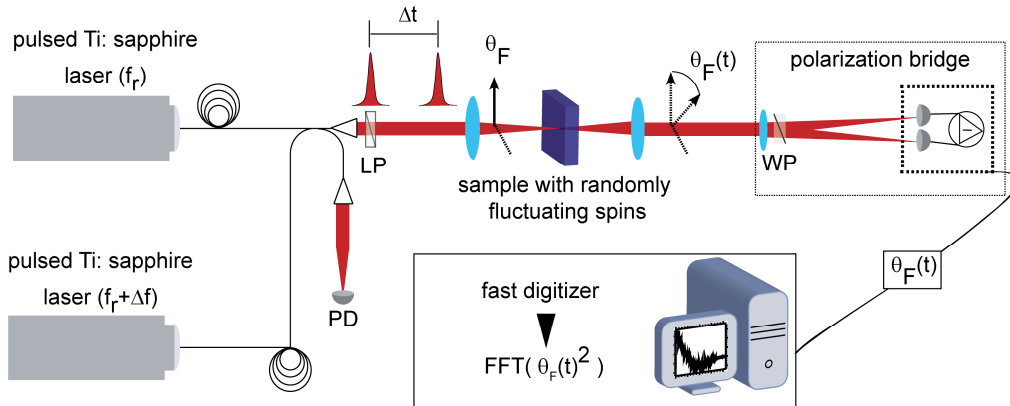

Fig. 1. Experimental set-up: The outputs of two degenerate ultrafast ps-laser oscillators are joined in a single mode, polarization maintaining optical fiber. A fast photodiode picks up the temporal evolution of Δt. The linear polarized fiber output is focused to a spot diameter of about 40 µm onto the sample which is mounted in a low temperature magneto-optical cryostat. The average power is 8 mW at a wavelength of 825 nm. The polarization axis of the transmitted linear probe light is analyzed by a polarization bridge. The difference signal is electrically amplified and sent to a PC for digitalization and further data processing.

In each period of $1/f_r = 12.5\,\text{ns}$ a pulse pair with a time delay changing by $\Delta t = \Delta f /[(f_r + \Delta f)f_r]$ samples the stochastic spin orientation at an arbitrary point in time t_i. The maximum time delay is $1/(2f_r) = 6.25\,\text{ns}$. In an ideal experiment the limited speed of the electro-optic conversion of the photoreceiver averages the Faraday rotation angle θ_F of both pulses contained in a pulse pair but resolves subsequent pulse pairs, i.e., an ideal receiver would have a top hat shaped passband up to 80 MHz such that the contribution of each pulse pair is summed to $\theta_F(t_i) + \theta_F(t_i + \Delta t_i)$ due to the capped time resolution, but subsequent events are not averaged. In our investigated sample the spin coherence time is much shorter than $6.25\,\text{ns}$ and thus every new cycle the phase of the spin dynamics is in good approximation fully arbitrary. Nevertheless, a pulse pair with a fixed delay Δt samples the stochastically varying fluctuation *amplitude* corresponding to the fluctuation envelope of the spin dynamic.

The sampling of the spin noise amplitude is exemplarily shown in Fig. 2 (left column) for an applied magnetic field invoking a Larmor precession of the spins. For clarity, the phase of the spin dynamic is kept constant and dephasing is neglected in the schematic. The middle column displays the individual signals of each pulse within a pulse pair and the right column shows the sum of both pulses which is detected by the photoreceiver. For a realistic spin noise signal the phase of the stochastic spin polarization is arbitrary at each cycle. However, the

variance of the stochastic noise amplitude changes with Δt as shown in the right column. The variance of the Faraday rotation angle $\left\langle [\theta_F(t_j) + \theta_F(t_j + \Delta t_j)]^2 \right\rangle$ thus contains all information about the temporal spin dynamics [14]. The continuous STUD-SNS signal $S_B(t)$ detected on a balanced receiver with a bandwidth b is given by:

$$S_B(t) = \int\limits_{t-b^{-1}/2}^{t+b^{-1}/2} \sum_{n=-\infty}^{\infty} \left[\delta(\hat{t} - f_r^{-1} \cdot n) + \delta(\hat{t} - (f_r + \Delta f)^{-1} \cdot n) \right] \times \left[\theta_F(\hat{t}) + \sigma(\hat{t}) \right] d\hat{t}. \quad (1)$$

Here, $\sigma(t)$ denotes the white photon shot noise and $\theta_F(t)$ the Faraday fluctuation signal. Both quantities are stochastically distributed around zero and the averages are zero, but the variances are finite. A more lucid form of Eq. (1) is obtained if only exactly the two pulses in a pulse pair are considered. This is a good approximation for spin coherence times which are significantly shorter than $1/f_r$. The temporal basis can be rewritten in terms of the relative delay $n \cdot \Delta t$ with n being an integer ranging between zero and $n_{max} = (2 f_r \cdot \Delta t)^{-1}$:

$$\{S_B(n \cdot \Delta t)\}^2 \propto \theta_F(t_i = 0) \cdot \theta_F(t_i = 0 + n \cdot \Delta t) + const. \quad (2)$$

All terms and cross-terms which do not explicitly depend on the correlation between $\theta_F(t_i = 0)$ and $\theta_F(t_i = 0 + n \cdot \Delta t)$ add up to a constant which is independent of Δt. The choice of $t_i = 0$ is legitimate since t_i is fully arbitrary. From Eq. (2) it now becomes clear that the full bandwidth of the STUD-SNS technique is given by $1/\Delta t$ with a fixed frequency resolution of $(\Delta t_{max})^{-1} = 2 f_r$ arising from the discrete Fourier theorem. A higher frequency resolution is thus possible with a lower repetition rate f_r. Interestingly, STUD-SNS is resolution limited but bears a potentially extremely high bandwidth given by the inverse sampling pulse width Δt_P, e.g., $(100 \text{fs})^{-1} = 10\,\text{THz}$ (!), which is complementary to the method presented in [4]. being bandwidth limited but reaching in principle an arbitrarily high resolution.
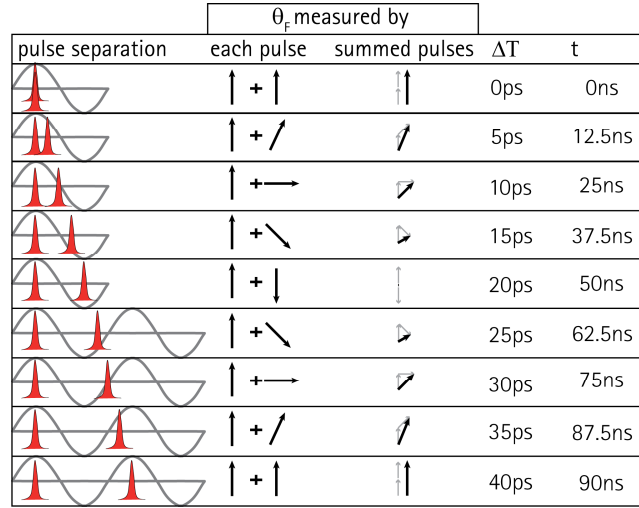
	θ_F measured by			
pulse separation	each pulse	summed pulses	ΔT	t
	↑ + ↑	↕	0ps	0ns
	↑ + ↗	↗	5ps	12.5ns
	↑ + →	↗	10ps	25ns
	↑ + ↘	▷	15ps	37.5ns
	↑ + ↓	↑	20ps	50ns
	↑ + ↘	▷	25ps	62.5ns
	↑ + →	↗	30ps	75ns
	↑ + ↗	↗	35ps	87.5ns
	↑ + ↑	↕	40ps	90ns

Fig. 2. STUD spin noise principle. The left column shows the continuously varying pulse delay Δt together with an exemplary spin Larmor precession. The second column displays the Faraday rotation θ_F sampled by each individual pulse leading to the detected Faraday rotation signal shown in the third column. In this example the detuning frequency is $\Delta f \approx 32\,kHz$.

An exciting feature of this technique for spin lifetimes shorter than a quarter of the laser repetition period is that a background spectrum containing only photon shot noise contributions is already included in one delay cycle. Figure 3 illustrates this intrinsic and fast background acquisition which avoids the need of any magnetic field sweeping or switching of polarization components [15] to discriminate the small spin noise signal from all other noise contributions. The first and last sections of the delay cycle contain the spin correlation signal, i.e., the envelope of the spin noise signal. The two middle sections contain only residual noise which is ideally composed of white noise only, including white spin noise, giving rise to the constant in Eq. (2). We want to point out that a strong increase in the spin coherence time would reduce the detected spin noise power due to an overlap of signal and background contributions. For very short spin coherence times τ_c the measured integrated spin noise power P_{SNS} also drops towards zero because $\theta_F(t_i)$ and $\theta_F(t_i + \Delta t)$ tend to be fully uncorrelated and thus contain the same white spin noise as the background data which has to be considered if f_r is fixed by the available laser sources. Figure 3(b) depicts a full numerical simulation (dots) of the spin noise signal. The measurable spin noise power P_{SNS} is maximal if both effects have their smallest impact which holds for τ_c being about half the signal window time. The numerical results can also be approximated by an analytical expression (red line) based upon a pseudo-Voigt type model $g(\Delta t, \tau_c(\eta), \eta) = \eta \cdot d_h + (1-\eta)d_i$. The model contains the weighted contribution of an inhomogeneous $d_i \propto e^{-(\Delta t/2\tau_c)^2}$ and a homogenous $d_h \propto e^{-\Delta t/\tau_c}$ spin decoherence type distribution. The integrated, i.e., for infinitesimal small Δt, measurable spin noise power is calculated analytically with $T_r = f_r^{-1}$ by

$$P^{SNS}(\tau_c(\eta)) \cdot P_{signal}^{SNS}\Big|_{\tau_c \to \infty} = \overbrace{\int_0^{T_r/4} g(\Delta t, \tau_c(\eta), \eta)\, d\Delta t}^{P_{signal}^{SNS}} - \overbrace{\int_{T_r/4}^{T_r/2} g(\Delta t, \tau_c(\eta), \eta)\, d\Delta t}^{P_{background}^{SNS}}. \qquad (3)$$
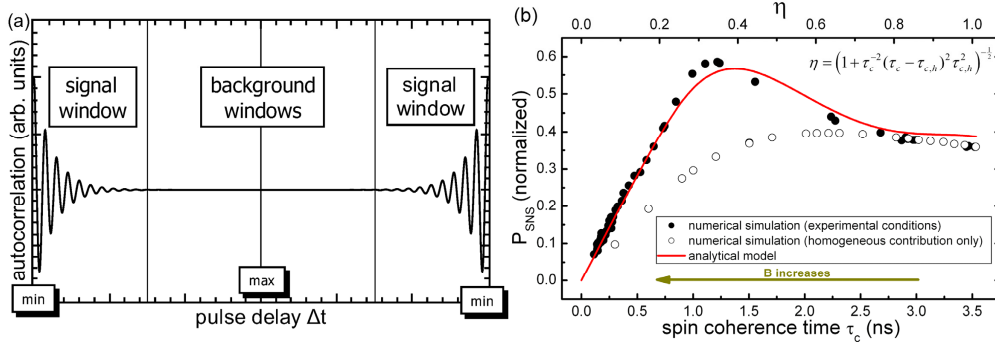

Fig. 3. (a) Illustrated is the SN autocorrelation at finite magnetic field for a full cycle of pulse pair delays. Δt periodically changes between its minimal and maximal value. The first and last sections contain the equivalent autocorrelation signal, whilst the two middle sections only contain photon shot noise. (b) Depicted is the dependence of the integrated spin noise power on the effective spin dephasing time as a result of a full numerical simulation of the experiments (dots) in units of the complete spin noise power for $\tau_c \to \infty$. The red line follows the analytical model assuming a pseudo-Voigt type weighted distribution (see text). The parameter η denotes the relative weight of in- $(\eta = 0)$ and homogenous contribution $(\eta = 1)$.

The simulations are fully numerically performed with an ensemble of 10^3 spins with a g-factor inhomogeneity $\sigma_g = 0.2\%$ and a homogenous spin lifetime $\tau_{c,h} = 3.5$ ns by a purely stochastic and independent evolution of the spin dynamics of each single spin. The analytical model and the simulated data depicted in Fig. 3(b) show very good agreement. Deviations in

the regime of strongly mixed contributions of the homo- and inhomogeneous spin decay are attributed to the Voigt-approximation made in the analytical expression and the slight discrepancy for long τ_c are related to an underestimation of the total spin noise power by the discrete FFT for spectrally very narrow signals. The connection between the relative weight η and the Voigt FWHM $w_v = (\pi \tau_c)^{-1}$ is approximated by $w_v^2 = (\pi \tau_{c,h})^2 + w_g^2$ with the Gaussian FWHM w_g linearly decreasing with η.

3. Measurement results

The data acquisition in the measurements is organized as follows: The electrically amplified signal from the balanced receiver is acquired by a fast digitizer card, which is synchronized with the master laser oscillator. The division into the four windows according to Fig. 3 is implemented on a personal computer and the point in time for the pulse pair with minimal delay is obtained by a fast photodiode having a responsivity depending on Δt. Power spectra obtained by fast Fourier transformation (FFT) "remove" the arbitrary phase of the spin noise signal and yield the spectral information only. The difference frequency Δf is adjusted such that half a delay cycle consists of $n_{max} = 2^k$ pulse pairs. This condition provides an optimal array size for performing the subsequent FFT and processing the optimal amount of information since each pulse pair constitutes a sampling point in time. Averaging the spectra improves the signal to noise ratio. The data acquisition of the balanced detector signal and its FFT is performed seamlessly by a fast personal computer. This method is at least two orders of magnitude more powerful compared to the spectral analysis of the noise signal by a usual sweeping spectrum analyzer with regards to the data throughput and thus the measurement time for an adequate spectrum [16].

The Fourier transform of a mono-exponential decay of the spin coherence with a decay time of τ_s yields a Lorentzian like spin noise signal centered at the Larmor frequency ν_L. The inverse full width $\Delta \nu$ of the Lorentzian is linked to the spin coherence time via the relation $\tau_s = (\pi \Delta \nu)^{-1}$. Figure 4 displays an excerpt of the measured full spectral noise power density of n-doped bulk GaAs ($n_{Si} = 2.7 \cdot 10^{15}\,cm^{-3}$) at low temperatures (4 K) for different transverse magnetic field strengths. The complete spectrum covers up to $\Delta t^{-1} = 164\,GHz$. The Larmor frequency shows the expected linear dependency on the magnetic field with $g* = 0.38$ and reaches frequencies of up to 42 GHz which is only limited by the maximum achievable field strength, i.e., the experiment proves the applicability of STUD-SNS to measure ultrafast spin dynamics. Figure 4 also shows a decrease of the spin noise signal with increasing magnetic field. The cause of this decrease is manifold. First, the spin noise amplitude decreases with an increasing spin dephasing rate invoked by, e.g., an inhomogeneity of the Landé g-factor. However, in general this process leaves the integrated spin noise power untouched but worsens the signal to noise ratio. A second effect arises from the relative constant shift of the conduction band edge with respect to the probe photon energy due to the diamagnetic shift of the GaAs band edge with increasing magnetic field. This effect, however, should have only a minor contribution. Thirdly, the increase in the spin dephasing rate decreases the sampled spin noise power due to the sampling effect as discussed in the previous section. Nevertheless, the detected spin noise power in the measurements drops more drastically than the increase in the measured spin relaxation rate implies, which might be attributed to the joint impact of all effects discussed above but which could not be fully clarified in these measurements.
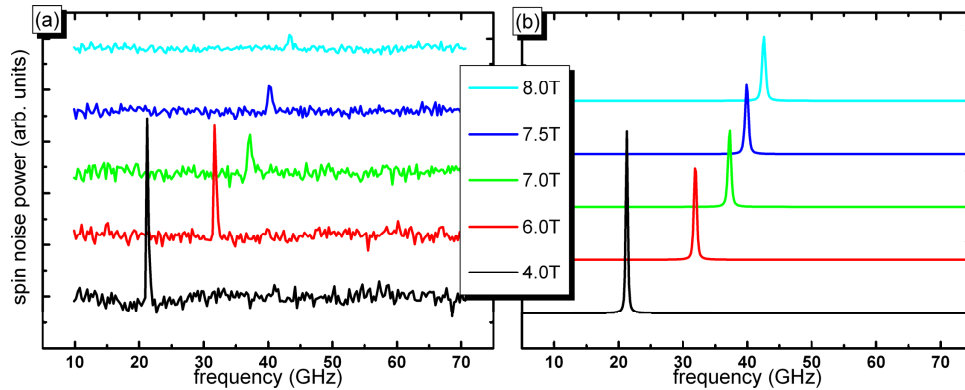
Fig. 4. (a) Experimental result of STUD-SNS. Shown is an excerpt of the measured spectral noise power density of n-doped bulk GaAs at low temperatures (4 K) for different transverse magnetic field strengths, i.e., Larmor frequencies. The difference frequency Δf is 39 kHz. The spin coherence time of $\tau_c \geq 1\,ns$ is determined by the spectral resolution of the setup and is in accordance with previously measured values of τ_c for this sample [3]. The measurement time for a single spectrum is 30 min. (b) Numerical simulations of the spin noise spectra. All spectra are vertically shifted for clarity.

4. Conclusion

We demonstrate for the first time the combination of the scanning temporal ultrafast delay technique with the quantum optical method of semiconductor spin noise spectroscopy. The effort of using two ultrafast oscillators is rewarded by an easy to implement background acquisition, yielding unambiguous signals not being affected by instabilities of the setup. As an archetypal and well understood model system we successfully applied STUD-SNS to measures the fast spin dynamics in moderately low doped GaAs. The high bandwidth of the presented STUD-SNS method is ideally suited for systems which intrinsically show a fast decay of spin coherence and are yet susceptible to optical excitation, like hole spin systems with a high degree of spin-orbit interaction [8]. An extension for measurements of extremely short spin lifetimes can be achieved by using two electronically phase-locked laser oscillators and only scanning the timespan comprising the relevant spin dynamics [17].